International Journal of Advances in Engineering and Management (IJAEM)
Volume 6, Issue 11 Nov. 2024, pp: 221-231 www.ijaem.net ISSN: 2395-5252

Experimental Assessment of a Refrigeration System Powered by a Gasoline Engine Utilizing Gasoline-Bioethanol Mixture

[1]Alajede A. M, [2]Olafimihan E.O, [3]Ogunsola A.D.[*].& [4]Sangotayo E.O.

[1,2,3,4,] *Department of Mechanical Engineering, Ladoke Akintola University of Technology, Ogbomoso, Nigeria,*

Date of Submission: 05-11-2024 Date of Acceptance: 15-11-2024

ABSTRACT
Dependable refrigeration is essential for vaccine preservation, especially in distant and resource-limited areas with unstable electrical supply. Gasoline-powered refrigeration systems present a viable option to electric-powered units; however, their efficacy and environmental consequences necessitate comprehensive assessment. This study investigated the experimental evaluation of a gasoline-powered refrigeration system featuring a micro-cooling compartment specifically intended for vaccine storage. Gasoline-bioethanol blends (E0, E5, E10, and E15) were evaluated in a four-stroke spark-ignition engine to enhance fuel economy and environmental sustainability. The physicochemical characteristics of these blends, such as pour point, octane number, cetane number, viscosity, density, carbon residue, and heating values, were examined to ascertain the optimal fuel composition. The system's effectiveness was estimated using COP.

The findings reveal that the E10 gasoline-bioethanol blend exhibited significant performance attributes, featuring appropriate octane ratings, viscosity, and density, alongside less carbon residue of 74% and an improved heating value of 410 MJ/kg and COP value of 12%. The employment of the E10 blend significantly reduced CO_2 emissions and enhanced engine performance, rendering it a viable fuel option for gasoline-powered refrigeration systems in this context.

This study emphasizes the promise of E10 as a more environmentally friendly and efficient fuel option for gasoline-powered refrigeration systems, enhancing engine performance and aiding in the reduction of carbon emissions. This research provides significant insights into sustainable refrigeration options for vaccine preservation in environments where conventional refrigeration is impractical, hence enhancing public health in neglected communities.

Keywords: Refrigeration, Heat Removal, Vapor-Compression System, Vaccine Preservation,

I. INTRODUCTION

Refrigeration is a process that entails the removal of heat by extracting heat from a confined environment or object to lower temperatures. In industrialized countries and wealthy areas of developing regions, refrigeration primarily functions to preserve food at low temperatures, effectively inhibiting the harmful effects of bacteria, yeast, and mold. This method permits numerous perishable items to be frozen, facilitating prolonged storage for months or even years, with minimum degradation of nutritional value, flavor, or appearance [1]. Refrigeration is an essential process in modern industrial and domestic environments, playing a critical role in sustaining optimal temperature levels for diverse uses and the vapor-compression system is the most often used approach owing to its efficiency and versatility [2]. Vaccination is essential for protecting the health of persons and animals against diseases by inducing the creation of antibodies, which are proteins that fight infections. The practice of vaccination is crucial for disease prevention in public health. The appropriate storage of vaccinations, especially in rural and distant areas, is a significant issue. Vaccines require stable and regulated temperature settings to maintain their efficacy, generally necessitating storage temperatures between 0°C and 8°C. Nonetheless, the difficulty emerges in regions lacking access to a national power grid,

International Journal of Advances in Engineering and Management (IJAEM)
Volume 6, Issue 11 Nov. 2024, pp: 221-231 www.ijaem.net ISSN: 2395-5252

where sustaining the necessary temperature for vaccine storage can be formidable. In these situations, vaccines sometimes require transportation from remote storage facilities to the place of use, which may involve problems and dangers during transit [3].

A study demonstrated the effective utilization of a tiny solar-powered refrigerator for cooling, achieving zero greenhouse gas emissions and the assembly included a Peltier module, heat sink, charge controller, solar panel, battery, and microcontroller kit, among other components [4]. A thermoelectric refrigeration system was designed and constructed in another study, with 12 Peltier modules, 5 DC fans, a refrigerator, and a freezer section. The Peltier modules were employed to chill the refrigerator sections, which were powered by an AC outlet. The system utilized 57 watts of electrical power. Following two hours of testing, the system exhibited a coefficient of performance (COP) of 81.85%, with compartment temperatures varying from 6.9℃ to -5.3℃ [5]. Sangotayo et al.[2] tested an adsorption refrigeration system using solar energy for heat gain. The system, consisting of a condenser, evaporator, adsorbent bed, and solar collector, and the findings revealed that temperatures of components increased by 25%, 4%, 13%, and 265% with solar time. The solar thermal-driven ARS showed satisfactory performance in Nigeria's southwestern climate, potentially replacing conventional refrigeration systems to mitigate global warming and environmental pollution. Isa et al. [6] identified several bacteria and fungi with differing efficiency in decomposing waste engine oil from gasoline and diesel cars, indicating possibilities for microbial remediation. The study concentrated on the microbiological deterioration of waste motor oil and did not examine the direct performance assessment of gasoline-powered refrigeration systems for vaccine preservation. Jereb et al. [7] demonstrated that CO_2 emissions peaked during vehicle idling and acceleration phases. Modifications to transportation infrastructure can diminish CO_2 emissions. The findings pertain to urban transit CO_2 emissions and interventions, without a specific emphasis on gasoline-driven refrigerated equipment for vaccine preservation.

Research also examined a vapor compression refrigeration system including an elliptical evaporator coil. Their research emphasized that modifying the evaporator's configuration and integrating expanded surfaces could improve heat transfer efficiency. The elliptical design led to a 1.5% enhancement in COP, attributed to an increased cooling effect and less compressor workload and heat absorption [8]. Bibri and Krogstie [9] elucidated the interplay between enhancements in energy efficiency and the mitigation of environmental pollutants in urban environments. Data-driven judgments are specific to each city. The study highlighted urban energy efficiency and environmental measures but did not provide a specific review of gasoline-powered refrigerated equipment for vaccine preservation. In another research study, scientists developed a mesoscale vapor compression refrigeration cycle utilizing R134A refrigerants in the form of VCRC. Their research produced a COP value of 3.34, indicating the system's efficacy in heat dissipation and cooling, appropriate for particular applications [10]. An author investigated a mesoscale VCRC employing R-134A and many other refrigerants. Their findings enhanced our comprehension of the design parameters required for particular evaporator heat loads [11]. An alternative method was the creation of an automotive air-conditioning system employing exhaust gas and vapor absorption refrigeration (VAR) technology. Their research demonstrated the viability of utilizing waste heat from car exhaust gasses to energize the VAR system, so obviating the necessity for an internal combustion engine and compressor.

Furthermore, an extensive study included the design of all elements of a refrigeration system, culminating in a compact CPU cooling unit. The utilization of R-134A refrigerant enabled effective heat dissipation and validated the practicality of an electric motor-driven isentropic compressor. The research also emphasized the possibility of a linear vapor compression compressor that operates without pistons, achieving a coefficient of performance (COP) of 3.0 [12]. Bulula et al. [13] reported that the entire expenditures for vaccine storage and distribution at MSD amounted to USD 1,996,286, while at EPI, the costs were USD 543,648. At MSD, distribution and program management costs constituted 41% (USD 819,288) and 38% (USD 762,968), but at EPI, storage and distribution costs accounted for 43% (USD 234,423) and 34% (USD 184,620). The study failed to include the potential inefficiencies and environmental ramifications linked to gasoline-powered refrigeration systems, which may affect long-term sustainability and cost-effectiveness. Haidari et al. [14] found that substituting vaccines with presentations having fewer doses per vial diminished vaccination availability by as much as 13% and escalated logistics costs by up to $0.06 per dose. Primary containers containing many doses per vial enhanced vaccination accessibility by 19% and decreased logistical expenses by $0.05

International Journal of Advances in Engineering and Management (IJAEM)
Volume 6, Issue 11 Nov. 2024, pp: 221-231 www.ijaem.net ISSN: 2395-5252

per dose. The emphasis was mostly on vaccine vial dimensions and logistical expenses, neglecting the particular efficacy and energy efficiency of gasoline-powered refrigeration systems for vaccine storage.

Gan et al. [15] developed performance indices that assessed the efficiency of vaccine storage boxes, including cold storage efficacy. Positioning PCM bottles on all six corners of the box proved to be the most efficacious, yielding a total normalized value of 2.87. The cooling duration was markedly influenced by the ambient temperature. The investigation was performed under a controlled temperature range of 2–8°C, which may not accurately reflect the actual circumstances encountered by gasoline-driven refrigeration systems in various locations. Thielmann et al. [16] reported that following program participation, the average knowledge scores of physicians and practice assistants regarding appropriate vaccine storage and temperature objectives significantly improved. The study emphasized the enhancement of knowledge among medical personnel instead of explicitly assessing the performance or efficacy of Gasiline-powered refrigeration systems for vaccine preservation. Nouni et al. [17] indicated that rapid economic development and a rising population in India have resulted in increased energy demand. The road transport industry, which is mostly dependent on petroleum, considerably contributes to CO_2 emissions. Alternative fuels have been investigated for the decarbonization of the sector. The study investigated alternate fuels but failed to offer comprehensive insights into the efficacy of gasoline-powered refrigeration systems specifically for vaccine preservation.

Paramonova et al. [18] demonstrated an enhancement in industrial energy efficiency (IEE) via technology dissemination. Electric motor technologies were pivotal in IEE. The study concentrated on industrial electric motor systems and excluded gasoline-powered refrigeration systems for vaccine preservation. This study evaluated the performance of a petrol-powered refrigeration system utilizing a component from an automotive air-conditioning system to enable refrigeration. The compressor functions using a petrol engine, enabling a cooling temperature range of 0-8°C. The efficacy of disease prevention through vaccination is contingent upon the region's ability to uphold optimal storage conditions for vaccines. Areas with dependable vaccine storage capabilities can more effectively manage disease outbreaks. In regions without a centralized power infrastructure, reliance on distributed generation sources is crucial. This situation has initiated the present research, which focuses on the experimental performance assessment of a refrigeration system powered by a petrol engine.

II. MATERIALS AND METHODS

Materials and Equipment

The following materials and components were employed in this study: a 35-liter Bed Side refrigeration system, a 0.5mm thick aluminum light sheet, auto-based paint in the Ash color, a 16-gauge electrode, a capillary tube, a hose, fiber, resin, wheels, bioethanol fuel (quantity and composition), and refrigerant (R134a).

Construction and Development of a Compartment

The compact refrigeration module is comprised of three systems: a bio-ethanol engine, an automotive air conditioner, and vaccine storage. The bio-ethanol generator is directly coupled to the automotive air conditioner. The refrigeration unit that is employed is a modification of the original components of an automotive vapor-compression air-conditioning system, which include a compressor, condenser, expansion valve, and evaporator, as well as an oil chiller and oil separator. The exchange of heat between the condenser and evaporator occurs through the movement of air streams. The thermostatic sort of expansion valve is utilized. R-134a will be selected as the refrigerant for this investigation. The indoor coil, which functions as an evaporator, absorbs heat from the fan-driven air stream as the refrigerant travels through it, thereby providing cooling. The refrigerant is introduced to the outdoor coil following compression, where it dissipates heat into an additional air stream. The automotive air conditioning system is capable of operating in a refrigeration cycle.

A 4-stroke, single-cylinder gasoline engine with a power output of 5 to 10 horsepower was employed. The refrigeration compressor was powered by this engine, which provided the mechanical energy required. The engine's I.C. brake output is determined by Equation (1)

$$PB = T\omega \qquad (1)$$

ω is the angular speed in radians per second (rad/sec.)

$$\text{But,} \quad \omega = \frac{2\pi N}{60}$$

$$\text{Thus,} P_B = 2\frac{\pi N}{60} \cdot T \qquad (2)$$

Equation 3 gives the expression for the brake thermal efficiency.

International Journal of Advances in Engineering and Management (IJAEM)
Volume 6, Issue 11 Nov. 2024, pp: 221-231 www.ijaem.net ISSN: 2395-5252

$$\eta_b = \frac{P_B}{mf \cdot CV} \qquad (3)$$

Where P_B is the brake power in watts, m_f is the mass flow rate of the fuel by this engine in kg/s, CV is the heating value used by this engine in J/kg.

Refrigeration System

The refrigeration system is presented in Figure 1 and it comprises a compressor, refrigerant, heat exchangers, and condenser. Figure 2 illustrates the orthogonal and Isometric view of the refrigeration system as well as the various perspectives (front, end, and top).

i. Refrigeration Compressor - a reciprocating compressor that is hermetically sealed and compatible with the engine's power output was chosen. The refrigerant's pressure and temperature were increased by compressing it with the compressor.
ii. Refrigerant - R134a, an environmentally benign refrigerant, was used to charge the system. This was charged by the system's specifications.
iii. Heat Exchangers - These were employed to transfer heat from the refrigerated chamber to the external environment.
iv. Condenser - A condenser that is air-cooled and has an adequate heat rejection capacity was employed. The purpose of this was to transfer heat from the refrigerant to the ambient air.
v. Evaporator - A fin-tube-type evaporator was implemented. This functioned to absorb heat from the refrigerated space.
vi. Thermostatic Expansion Valve (TXV): A Thermostatic Expansion Valve (TXV) was installed. This regulated the passage of refrigerant into the evaporator.
vii. Refrigeration Chamber: This is an insulated chamber with a volume of approximately 1-2 cubic meters that was employed. This functioned as the experiment's cooling compartment.

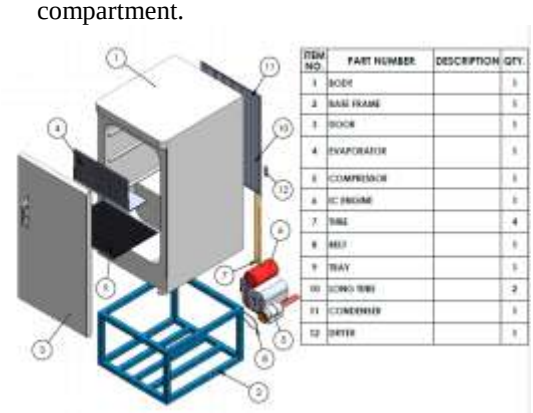

Figure 1: Refrigeration System

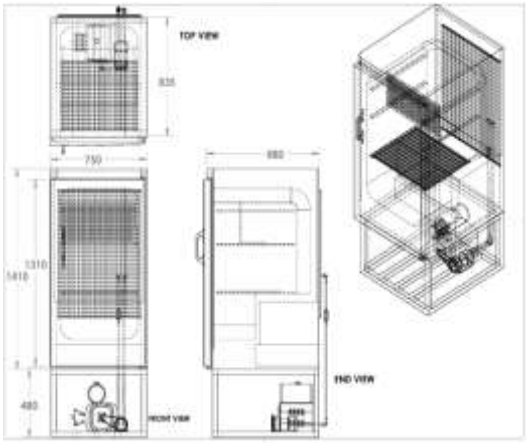

Figure 2: Orthogonal and Isometric View of the Refrigeration System

METHODOLOGY FOR SYSTEM ASSEMBLY

A suitable coupling or belt drive system was employed to connect the refrigeration compressor to the gasoline engine during the system's assembly. The compressor discharge line was connected to the condenser intake using copper tubing. The evaporator inlet was connected to the expansion valve outlet, and the condenser outlet was connected to the expansion valve inlet. The compressor suction line was reconnected to the evaporator output. To guarantee that all connections were secure and leak-proof, they were examined. A vacuum pump was employed to evacuate the system, thereby eliminating any moisture and air. The system was subsequently primed with the refrigerant (R134a).

EVALUATION OF PERFORMANCE

The gasoline engine's vital parameters, including compressor suction and discharge pressures, temperatures at critical locations, refrigerant flow rate, and fuel consumption rate, were monitored and recorded. The system's cooling capacity was determined by analyzing the temperature and flow rate data that was collected. Equation 4 was employed to calculate the Coefficient of Performance (COP).

$$COP = \frac{\text{Cooling Capacity (kW)}}{\text{Engine Power Input (kW)}} \qquad (4)$$

The Gasoline-driven refrigeration system's efficacy was assessed through data analysis.

Data Analysis

The data logger was employed to acquire data on temperature, pressure, and flow rate during the testing period. Fuel consumption was

International Journal of Advances in Engineering and Management (IJAEM)
Volume 6, Issue 11 Nov. 2024, pp: 221-231 www.ijaem.net ISSN: 2395-5252

periodically monitored. The cooling capacity, COP, and fuel efficiency were calculated. The theoretical predictions were contrasted with the experimental results. The data was analyzed to identify trends, including the influence of engine strain on system performance.

III. RESULT AND DISCUSSION

Micro Cooling System Assembly Developed

The microcooling system is a specialized assemblage that is intended to maintain the optimal temperature necessary for its preservation. Figure 3 illustrates the assembly of the microcooling system that was developed. The assembly comprises the following components: the insulated compartment, cooling unit, temperature control system, data logging and monitoring, evaporator outlet and blower motor with protective cover, condenser with fan, dryer, alternator, freezer compartment, base and base tire, vaccine tray, and working substance (refrigerant).

The insulated compartment at the heart of the micro-cooling system is designed to reduce the transfer of heat from the external environment. The thermal insulation materials used in the construction of this compartment are of the highest quality, ensuring that the internal temperature remains consistent regardless of the variable ambient conditions. In the same vein, the cooling device was engineered to effectively cool the air within the compartment, thereby guaranteeing that the temperature remains within the acceptable range for vaccine storage. The cooling unit is energy-efficient, enabling it to operate for an extended period without consuming an inordinate amount of power. Furthermore, a precise temperature control mechanism was implemented, which encompassed digital thermostats and sensors. The cooling output is adjusted by the internal temperature, which is continuously monitored by these components. This guarantees that any deviations from the desirable temperature range (typically between 2°C and 8°C) are promptly rectified, thereby ensuring dependable preservation conditions. The system also incorporates data logging capabilities to improve safety and compliance. This function documents temperature fluctuations over time, enabling users to monitor the vaccines' storage conditions.

The micro refrigeration system can be operated on a variety of power sources, such as AC mains and battery backup, by incorporating a gasoline-bioethanol blend. This adaptability guarantees that the immunizations can be preserved in regions with intermittent electricity supply, rendering them appropriate for use in remote areas or during emergencies. The gasoline-driven refrigeration system for vaccine preservation (Figure 3) is a critical innovation in the healthcare sector that guarantees the optimal storage and transportation of vaccines. It is a critical instrument for preserving the efficacy of vaccines, thereby contributing to public health and safety, due to its robust design and precise temperature control.

Figure 3: Assemblage of Gasoline-driven Refrigeration System

Physicochemical Properties of Gasoline-Bioethanol Blends

The values of each physicochemical property were subject to fluctuations as the volume percentage of ethanol in the mixtures increased, as illustrated in Figures 4 to 12. The gasoline-bioethanol combine exhibited an increase in density, viscosity, heating values, and specific gravity. This phenomenon can be attributed to a variety of factors that are associated with the properties of ethanol and its interaction with fuel.

The graph of Octane numbers against blending ratios is depicted in Figure 4. The fuel mixture's overall octane rating decreases from 0 to 6%, while the octane number increases when ethanol is combined with gasoline in a blend ratio that increases from 6% to 15%. At a blend ratio of 6%, the minimum octane number is 8°C. This is particularly beneficial in high-compression engines, which require fuels with a higher octane rating to prevent ringing. Ethanol burns at a lower temperature and consumes at a slower rate than gasoline, which can lead to a more controlled combustion process. The blend's effective octane rating is enhanced by this attribute, which reduces the likelihood of pre-ignition and clanging.

International Journal of Advances in Engineering and Management (IJAEM)
Volume 6, Issue 11 Nov. 2024, pp: 221-231 www.ijaem.net ISSN: 2395-5252

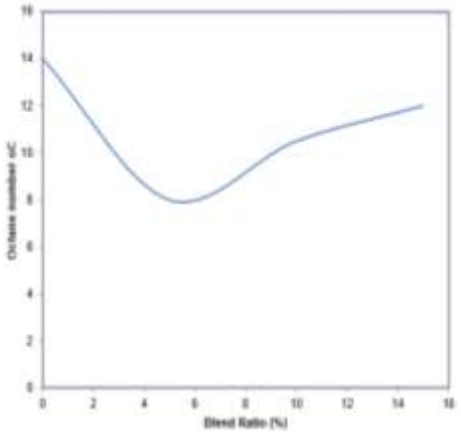

Figure 4: Graph of Octane Number against Blending Ratios

Figure 5 illustrates the relationship between Viscosity in centipoise at 20 °C and blending ratios. The Viscosity of the fuel mixture escalates from 0 to 6%, followed by a decline as ethanol is incorporated with gasoline, increasing the blend ratio from 6% to 15%. At a blend ratio of 6%, the Viscosity reaches a peak of 14 centipoise. Furthermore, ethanol exhibits a higher viscosity than petroleum. The overall viscosity of the fuel mixture rises with blending (Figure 5). This alteration may impact the engine's combustion characteristics and fuel atomization. Additionally, temperature influences fuel viscosity; ethanol may exhibit greater viscosity than pure gasoline in colder conditions, potentially affecting engine performance and fuel delivery. Nonetheless, viscosity may stabilize at operational temperatures, although the compound will still possess a higher viscosity than gasoline alone.

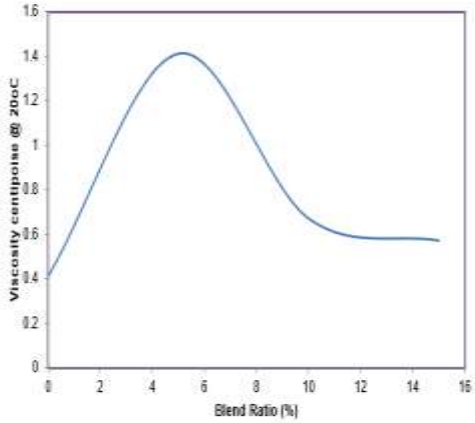

Figure 5: Graph of Viscosity centipoise @ 20 °C against Blend Ratio (%)

Figure 6 depicts the graph of Flashpoint in relation to blending ratios. The total flashpoint of the fuel mixture diminishes from 0 to 6%, however the flashpoint rises when ethanol is blended with gasoline in ratios increasing from 6% to 15%. At a mix ratio of 6%, the minimum flashpoint is 25°C. The total flash point of the mixture rises with blending, making it less volatile than pure gasoline. This can enhance the safety of storage and handling. The integration of ethanol into gasoline is expected to alter the volatility characteristics of the fuel. The use of ethanol can reduce the volatility of gasoline's lighter components, leading to an increased flash point for the blend. This alteration may reduce the likelihood of vapor lock and improve safety in high-temperature scenarios.

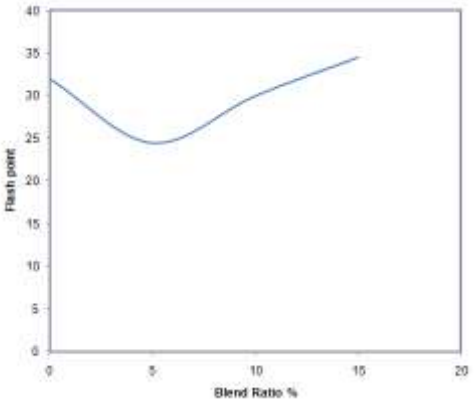

Figure 6: Graph of Flashpoint against Blending Ratios

Figure 7 depicts the correlation between density and blending ratios. The density of the fuel mixture increases from 0 to 6%, then decreases when ethanol is blended with gasoline, raising the blend ratio from 6% to 15%, at a blend ratio of 6%, the density attains a maximum of 0.89 kg/L. The addition of ethanol to gasoline decreases the overall density of the fuel mixture (Figure 7). The reduction in density may affect fuel delivery and combustion characteristics within the engine. As the concentration of ethanol in the mixture increases, the total density of the fuel decreases further. This may lead to changes in the volumetric flow rate of gasoline, thus affecting the engine's performance and efficiency. Subsequently, a rise in the density of the combination was seen.

International Journal of Advances in Engineering and Management (IJAEM)
Volume 6, Issue 11 Nov. 2024, pp: 221-231 www.ijaem.net ISSN: 2395-5252

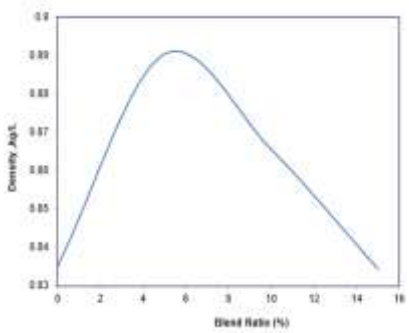

Figure 7: Graph of Density (kg/L) against Blend Ratio (%)

Figure 8 illustrates the graph of carbon residue in relation to blending ratios. The overall carbon residue of the fuel mixture decreases from 0% to 10%; however, the carbon residue increases when ethanol is combined with gasoline in proportions ranging from 10% to 15%. At a mixing ratio of 10%, the lowest carbon residue is 74%. Ethanol possesses a lower carbon and higher oxygen content compared to gasoline, which diminishes carbon residue at reduced blend ratios; nonetheless, the gasoline's elevated carbon content prevails in the mixture at lower ethanol concentrations. The blend containing 10% ethanol attains the minimal Carbon residue (74%), signifying ideal mixing; nevertheless, exceeding 10% ethanol may result in the introduction of more complex molecules, hence elevating Carbon residue. Lower carbon residue correlates with diminished particulate matter and CO_2 emissions, whereas proper blending ratios improve engine efficiency and decrease maintenance requirements.

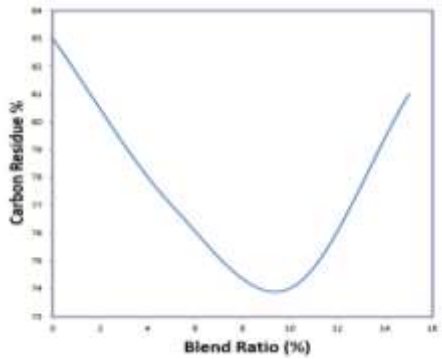

Figure 8: Graph of Carbon residue against Blend Ratio (%)

Figure 9 illustrates the relationship between Specific Gravity (SG) and blending ratios. The specific gravity of the fuel mixture rises from 0 to 6%, then declines when ethanol is incorporated with gasoline, increasing the blend ratio from 6% to 15%. At a blend ratio of 6%, the specific gravity reaches a peak of 0.85. The alterations in specific gravity influence fuel density, viscosity, and combustion properties; ideal blending ratios improve engine efficiency, power output, and emissions and comprehending the correlations of SG-blend ratios aids in the refinement of fuel specifications. The potential causes for the reduction in specific gravity beyond a 6% blend ratio include suboptimal interactions between ethanol and gasoline at elevated concentrations, the surplus of ethanol potentially increasing volume and thereby decreasing overall density, and alterations in molecular arrangements that may influence the density of the mixture.

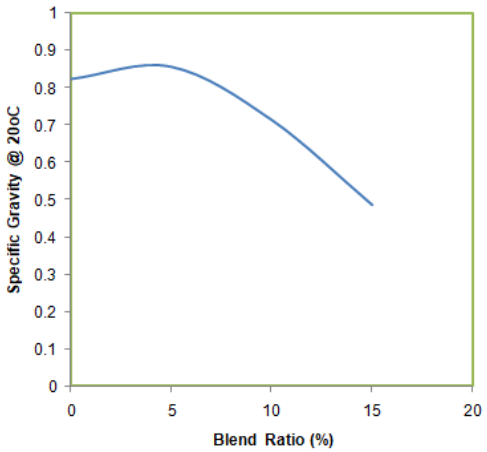

Figure 9: Graph of **Specific Gravity @ 20oC against Blend Ratio (%)**

The correlation between blending ratios and pour point oC is illustrated in Figure 10. The fuel mixture's pour point oC is subject to fluctuations as the blend ratio increases from 0% to 15%. At a blend ratio of 10%, the pour point oC reaches a maximum of 8oC. It elucidates that the Pour Point of the blend is influenced by the reduced viscosity and higher volatility of ethanol. The blend is dominated by the properties of gasoline at lesser ethanol concentrations (0-5%). The Pour Point increases as the ethanol content (5-10%) increases due to the interactions between ethanol and gasoline molecules. Optimal mixing is indicated by the blend's optimum Pour Point (8°C) at 10% ethanol. Pour point decreases beyond 10%: The Pour Point may be reduced by the addition of additional ethanol (10-15%), which may be the result of the excess ethanol disrupting molecular interactions. It suggests that fuel flowability is influenced by Pour Point, particularly in colder temperatures. Reliable engine operation is

International Journal of Advances in Engineering and Management (IJAEM)
Volume 6, Issue 11 Nov. 2024, pp: 221-231 www.ijaem.net ISSN: 2395-5252

guaranteed by the optimal blending ratios, and the comprehension of Pour Point-blend ratio correlations informs fuel storage and management practices.

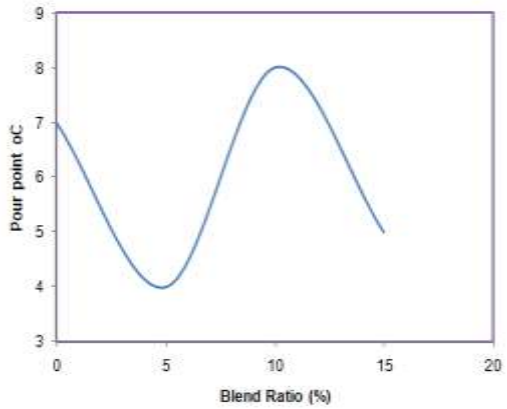

Figure 10: Graph of Pour point oC against Blend Ratio (%)

Figure 11 illustrates the relationship between Cetane number and blending ratios. The Cetane number of the fuel mixture demonstrates variability as blend ratios increase from 0% to 15%; at a blend ratio of 10%, the Cetane number reaches a peak of 15°C. The higher octane rating and lower cetane number of ethanol influence the Cetane rating of the blend. At lower ethanol concentrations (0-5%), the characteristics of gasoline prevail in the mixture; as ethanol content rises (5-10%), interactions between ethanol and gasoline molecules result in an elevated Cetane Number. The blend attains the highest Cetane Number at 10% ethanol, signifying optimum amalgamation. A greater Cetane Number enhances gasoline ignition quality and diminishes engine knocking, and proper blending ratios facilitate efficient combustion and lower emissions.

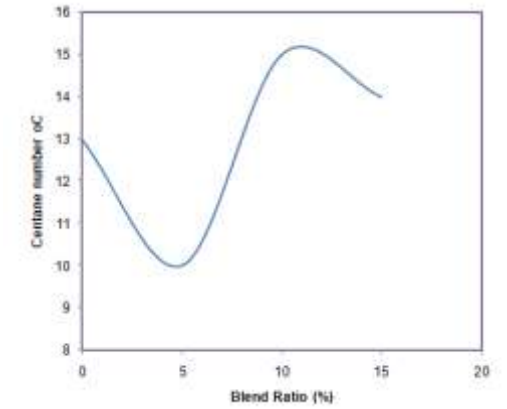

Figure 11: Graph of Cetane number oC against Blend Ratio (%)

Figure 12 illustrates the graph of heating values with blending ratios. The heating values of the fuel mixture increase from 0 to 10%, but they decrease as the ratio of ethanol to gasoline increases from 10% to 15%. When the blend ratio is 10%, the maximum heating value is 410 MJ/kg. The correlation between the higher and lower thermal values of gasoline-bioethanol compounds is illustrated in Figure 12. The energy content of the E10 gasoline-bioethanol blend is indicated by its greatest heating value (410-412 kJ/kg). This is equivalent to assessing the efficacy of various mixtures to improve fuel efficiency and power output. The thermal value of the composite decreases as E15 bioethanol is incorporated into gasoline. This may be attributable to the blend's exceptionally low energy value. The efficacy of combustion may also be influenced by the reduction in heating value. It may be necessary to make adjustments to the timing and fuel injection to enhance the performance of engines that operate with a lower-energy mixture. This can result in complete combustion and an additional increase in efficiency if the calibration is precise. The total thermal value of the blend is reduced as a result of the dilution effect of the lower-energy ethanol, which is a consequence of the incorporation of ethanol into gasoline (Figure 12). The efficacy of combustion may also be affected by the decrease in heating value. Modifications to fuel injection and timing may be necessary to improve the performance of engines with the lower-energy mixture. If precisely calibrated, this can lead to complete combustion and an additional increase in efficiency.

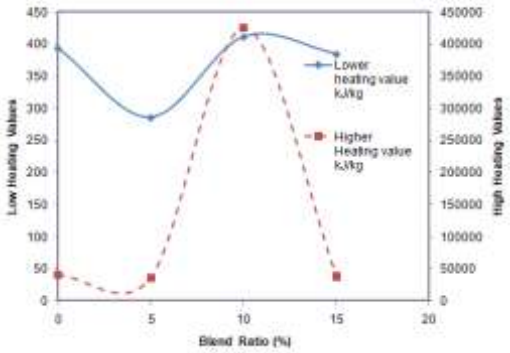

Figure 12: Graph of Heating Values against Blend Ratio (%)

Characterization of Engine Test ResultsforE0, E5, E10 and E15 Blends

International Journal of Advances in Engineering and Management (IJAEM)
Volume 6, Issue 11 Nov. 2024, pp: 221-231 www.ijaem.net ISSN: 2395-5252

The outcomes of speed, torque, brake power, brake thermal efficiency, and COP generated by the four-stroke spark-ignition engine test rig. The findings are displayed in Figures (13-15) The acquired result served as a reference for determining the test performance parameters of the engine test rig for the gasoline-bioethanol combination. Figure 13 presents the outcomes of torque (Nm), Figure 14 depicts braking power (kW), and Figure 15 displays brake thermal efficiency (%) and COP generated by the engine test rig operating on a specific gasoline-bioethanol blend at a constant speed of 356.19 rad/sec.

Analyzing the test performance parameters of an engine functioning at a consistent speed of 356.19 rps, while varying torque, braking power, and brake thermal efficiency values.

The E15 gasoline-bioethanol blend exhibits a reduced torque output of 9.8 Nm, in contrast to the E10 gasoline-bioethanol blend, which produces 10.8 Nm. This signifies that the engine can generate greater rotational force in the third scenario, potentially enhancing acceleration and overall performance. The brake power of the E0 gasoline-bioethanol blend is 373.00 W, but the E5 gasoline-bioethanol blend produces 384.19 W, the E10 blend yields 391.65 W, and the E15 blend generates 365.54 W.

Figure 13 demonstrates that torque (Nm) decreases as the proportion of gasoline to bioethanol rises. Bioethanol exhibits a lower energy density (~26.7 MJ/kg) than gasoline (~44.4 MJ/kg), and the presence of oxygen in ethanol may result in a somewhat reduced energy release after combustion.

The diminished torque leads to a reduction in engine power and performance, while lower energy density and modified combustion parameters may affect fuel efficiency, resulting in decreased acceleration and responsiveness perceived by personnel.

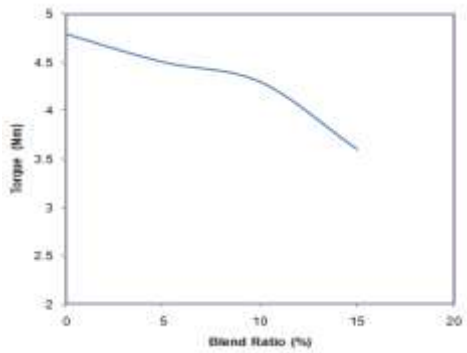

Figure 13: Graph of Torque (Nm) against Blend Ratio (%)

Figure 14 depicts the correlation between Brake Power (kW) and the gasoline-to-bioethanol blend ratio.

Brake Power (kW) diminishes as the bioethanol mix ratio escalates, exhibiting a non-linear reduction characterized by a more pronounced decline at elevated bioethanol concentrations. It elucidates that bioethanol's reduced energy density (~26.7 MJ/kg) in comparison to gasoline (~44.4 MJ/kg) results in diminished Brake Power. Bioethanol's superior octane rating and combustion characteristics may result in a marginally reduced energy output during combustion. The factors contributing to diminished brake power include the reduced energy content of bioethanol. To sustain power, engines may need increased fuel, resulting in diminished efficiency, since bioethanol's elevated octane rating can induce engine knock or pinging, hence decreasing Brake Power. Decreased Brake Power adversely impacts vehicle acceleration, responsiveness, and overall performance; lower Brake Power results in diminished fuel efficiency, particularly at elevated bioethanol mix ratios, and the long-term effects of bioethanol combustion on engine components necessitate attention.

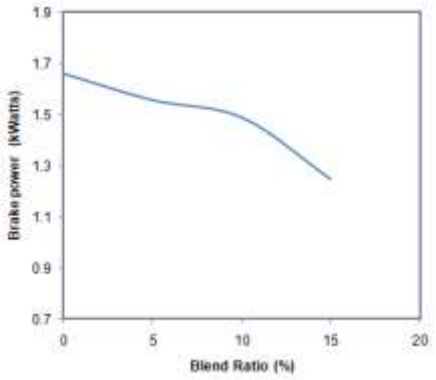

Figure 14: Graph of Brake power (kW) against Blend Ratio (%)

Figure 15 demonstrates that braking power efficiency diminishes linearly with an increase in the gasoline-to-bioethanol blend ratio. The coefficient of performance (COP) decreases as the gasoline-to-bioethanol blend ratio grows from 0% to 10%, whereas the COP value of 12% remains consistent with the blend ratio beyond 10%. The efficiency of braking power diminishes linearly with an increase in the bioethanol blend ratio, such that each percentage point increase in bioethanol results in a proportional fall in braking power efficiency. The coefficient of performance

International Journal of Advances in Engineering and Management (IJAEM)
Volume 6, Issue 11 Nov. 2024, pp: 221-231 www.ijaem.net ISSN: 2395-5252

(COP) diminishes as the bioethanol blend ratio escalates from 0% to 10%, whereas a stable COP is seen at about 6% for blend ratios over 10%. Bioethanol necessitates that engines adjust to the combustion characteristics of bioethanol at elevated mix percentages, and blends beyond 10% are formulated to improve performance and mitigate losses. Elevated bioethanol concentrations resulted in enhanced combustion efficiency, compensating for energy density reductions and the long-term impacts of bioethanol combustion on engine components necessitate evaluation. The results demonstrate that the brake power of the E10 gasoline-bioethanol blend, which measures the engine's output power after accounting for losses due to friction and other factors, attains a peak of 391.65 W. The augmented brake power in the E10 gasoline-bioethanol blend (8.16%) signifies that the engine is more efficient in converting fuel energy into useful work at the same speed.

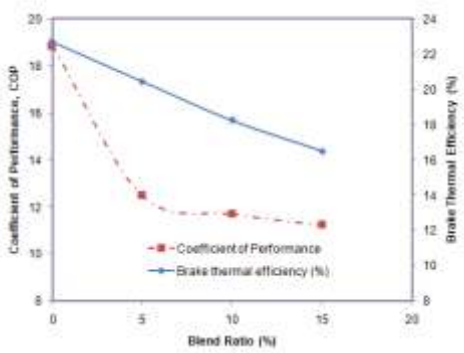

Figure 15: Graph of braking thermal efficiency and Coefficient of Performance (COP) of the system against Blend Ratio (%)

IV. CONCLUSIONS

The following conclusions were drawn from the present study on the performance evaluation of a gasoline-powered refrigeration system for vaccine storage as follows: A chamber was created to accommodate a micro-cooling device for vaccine preservation. The system's efficiency was evaluated using gasoline-bioethanol blends (E0, E5, E10, and E15) as options in a four-stroke spark-ignition engine to power the proposed refrigeration system. The physicochemical characteristics of gasoline-bioethanol blends (E0, E5, E10, and E15) were evaluated. The E10 gasoline-bioethanol blends demonstrate enhanced properties regarding Cetane number, pour point, viscosity, density, carbon residue, and heating values. The effect of bioethanol on braking power efficiency is uniform and linear. The coefficient of performance (COP) exhibits heightened sensitivity to bioethanol content at lower blend ratios (0-10%), whereas above 10% bioethanol, the COP stabilizes, suggesting a probable ideal blend ratio. The utilization of E10 gasoline-bioethanol mixtures in four-stroke spark-ignition engines will diminish CO_2 emissions and improve engine performance.

REFERENCES

[1]. Sahoo, M. and Rout, I. S.(2016) "Design, fabrication and performance analysis of solar PV air conditioning system", International Journals of Scientific and Research Publications, Vol.6, Issue.10, pp.277-282,

[2]. Sangotayo, E. O., Waheed, M. A., and Bolaji, B.O. (2018): Experimental Evaluation of a Thermally Driven Adsorption Refrigeration System in Ogbomoso Environs, Journal of Energy Technologies and Policy, ISSN 2224-3232 (Paper) Vol. 8, No. 5, pp12-20,

[3]. Ojo B. (2023) Design, Fabrication, and Performance Evaluation of a Petrol-Driven Refrigerating System for Effective Vaccine Storage in Remote Areas, World Academics Journal of Engineering Sciences 10(3), pp.53-63

[4]. Selvaraj M Elavarasan E, Babloo Kumar Sah , Chandan Kumar, Dhananjay Kumar Ram, Krishn Pratap Singh, (2018)" Design and Fabrication of Mini Solar Refrigerator," International Journal of Engineering Research and Technology, Vol.6, Issue.10, pp.1-4,.

[5]. Oghoghome Oghenkevwe and Okonma John, " Design and Fabrication of Thermoelectric Refrigerator," Global Scientific Journals, Vol.4, Isuue.3, pp. 265-277, 2023.

[6]. Isa, M. S. M., & Mazlan, A. Z. A. (2021, April). Hand-arm vibration transmissibility measurement from the gasoline-driven motorboat engine. In Journal of Physics: Conference Series (Vol. 1896, No. 1, p. 012006). IOP Publishing.

[7]. Jereb, B., Stopka, O., &Skrúcaný, T. (2021). Methodology for estimating the effect of traffic flow management on fuel consumption and CO2 production: a case study of Celje, Slovenia. Energies, 14(6), 1673.

[8]. J. Chandramouli, C. Sreedhar, E. Subbareddy, and P. Student, "Design, Fabrication and Experimental Analysis of Vapour Compression Refrigeration

System with Ellipse shaped Evaporator Coil," International Journal of Innovative Research in Science, Engineering and Technology, An ISO, vol. 3297, Issue.8, pp.7775-7782, 2015

[9]. Bibri, S. E., &Krogstie, J. (2020). Environmentally data-driven smart sustainable cities: Applied innovative solutions for energy efficiency, pollution reduction, and urban metabolism. Energy Informatics, 3(1), 29.

[10]. Chow L.C., Ashraf N.S., Carter III H.C., Casey K., Corban S., Drost M.K., Gumm A.J., Hao Z., Hasan A.Q., Kapat J.S., Kramer L., Newton M., Sundaram K.B., Vaidya J., Wong C.C., Yerkes K., "Design and analysis of a mesoscale refrigerator," Proceedings of the ASME International Mech. Eng. Congr. and Expos., ASME, pp.1-8, 1999.

[11]. Phelan P.E., Swanson J., Chiriac F., Chiriac V., "Designing a mesoscale vapor-compression refrigerator for cooling high-power microelectronics," 93 Proceedings of the Inter Society Conference on Thermal Phenomena, IEEE, pp.218-23, 2020.

[12]. Heydari A., "Miniature vapor compression refrigeration systems for active cooling of high-performance computers," Proceedings of the Inter Society Conference on Thermal Phenomena, IEEE, pp.371-378, 2019.

[13]. Bulula, N., Mwiru, D. P., Swalehe, O., & Mori, A. T. (2020). Vaccine storage and distribution between the expanded program on immunization and medical store department in Tanzania: a cost-minimization analysis. Vaccine, 38(51), 8130-8135.

[14]. Haidari, L. A., Wahl, B., Brown, S. T., Privor-Dumm, L., Wallman-Stokes, C., Gorham, K., ... & Lee, B. Y. (2015). One size does not fit all: the impact of primary vaccine container size on vaccine distribution and delivery. Vaccine, 33(28), 3242-3247.

[15]. Gan, Q., Zhang, Y., Zhang, Z., Chen, M., Zhao, J., & Wang, X. (2023). Influencing factors of cooling performance of portable cold storage box for vaccine supply chain: An experimental study. Journal of Energy Storage, 72, 108212.

[16]. Thielmann, A., Puth, M. T., &Weltermann, B. (2020). Improving knowledge on vaccine storage management in general practices: Learning effectiveness of an online-based program. Vaccine, 38(47), 7551-7557.

[17]. Nouni, M. R., Jha, P., Sarkhel, R., Banerjee, C., Tripathi, A. K., & Manna, J. (2021). Alternative fuels for decarbonization of road transport sector in India: Options, present status, opportunities, and challenges. Fuel, 305, 121583.

[18]. Paramonova, S., Nehler, T., &Thollander, P. (2021). Technological change or process innovation–An empirical study of implemented energy efficiency measures from a Swedish industrial voluntary agreements program. Energy Policy, 156, 112433.